1975, he has been a Professor of Electrical Engineering at the Technical University Munich, Munich, West Germany. His research interests are in computer-aided design of electronic circuits and systems, with particular emphasis on circuit optimization, layout synthesis, and fault diagnosis.

Dr. Antreich is a member of the NTG (Nachrichtentechnische Gesellschaft, Germany, the German Association of Communication Engineers). He received the NTG prize paper award in 1976. He was chairman of the NTG Circuit and System Group from 1972 to 1974. Since 1979, he has been member of the executive board of the NTG.

✦

Rudolf K. Koblitz was born in Worms, Germany on September 12, 1950. He received the Dipl. Ing. degree from the Technical University Darmstadt, Darmstadt, Germany, in 1976.

Since May 1976 he has been with the Department of Electrical Engineering, Technical University of Munich, Munich, Germany, working in the field of CAD, statistical design, and design centering of integrated circuits.

Mr. Koblitz is a member of the German Nachrichtentechnische Gesellschaft (NTG). He received the 1981 prize paper award from the German Nachrichtentechnische Gesellschaft.

Operational Amplifier Gain–Bandwidth Product Effects on the Performance of Switched-Capacitor Networks

RANDALL L. GEIGER, MEMBER, IEEE, AND EDGAR SANCHEZ-SINENCIO, MEMBER, IEEE

Abstract — A method of analyzing switched-capacitor (SC) filters which incorporates a single-pole model of the operational amplifiers (op amp's) is presented. Closed-form algebraic expressions for filter transfer functions in the z-domain are obtained which are computationally more efficient than time-domain methods. The necessity for including a frequency dependent model of the op amp rather than the common finite gain model in doing a performance analysis, especially when considering stability, is emphasized.

To illustrate the method of analysis, an analog integrator, an analog second-order bandpass filter, and their SC counterparts are considered. The s-domain performance of the analog circuits[1] is compared with the z-domain performance of the sampled-data configurations to show how the finite gain–bandwidth product (GB) of the op amp's affects the respective topologies. These comparisons show that the effects of switching rates and switching arrangements on filter performance are strongly dependent upon the GB product of the op amps. These comparisons also emphasize the fact that it is not sufficient to investigate the effect of the operational amplifiers on the performance of an analog filter to predict the performance of a SC filter derived from the analog configuration.

I. INTRODUCTION

THE EFFECTS of the finite gain–bandwidth product (GB) of the operational amplifier (op amp) on the performance of active filters has received considerable at-

tention [1]–[5]. The effects of GB on the performance of analog sampled data filters employing op amp's and switched capacitors (SC) are investigated here.

Several authors have recently presented systematic analysis procedures for obtaining closed-form expressions for the z-domain transfer functions of SC filters [7]–[11]. The op amp's have either been assumed to be ideal or to have a finite frequency independent gain in these analyses. Generally one of these two assumptions was standard when analyzing active RC filters up until the early 1970's at which time it was generally agreed that a frequency independent model of the op amp was inadequate. Since that time, the single-pole model of the op amp [2] has received widespread acceptance. One would suspect that it is equally important to include at least a single-pole model of the op amp when analyzing analog sampled-data filters. Such a model has been employed by Martin and Sedra [12] to analyze a SC integrator but their extension to second- and higher order networks is only possible for a special restrictive class of filter structures. Temes [13] has also used the single-pole model in the analysis of first-order networks.

A simple macromodel of an op amp employing two resistors, two capacitors, and three ideal op amp's is used which has input, output, and gain characteristics of an ideal op amp except for a single-pole at the origin. With the use of this macromodel, the influence of GB on SC filters can be determined.

The effects of the operational amplifier GB products on the transfer functions of two SC integrators are investi-

[1]A continuous-time circuit is referred to as an analog circuit. A sampled-data circuit is a switched-capacitor circuit here.
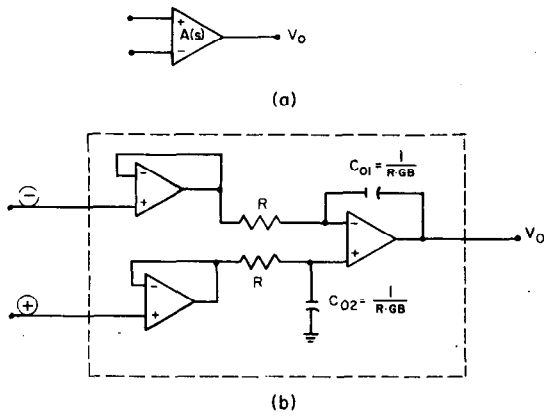
Fig. 1. A simple op amp macromodel. (a) Single-pole op amp. (b) Macromodel of op amp.

Fig. 2. Continuous time and sampled-data integrators. (a) Analog integration. (b) Bilinear z-transform integrator. (c) Forward z-transform integator.

gated in the z-domain. A continuous time second-order state variable filter is then transformed into a sampled-data filter by replacing the integrators by ones similar to the two sampled data integrators just mentioned. Root locus plots in the s-domain for the analog filter and in the z-domain for the sampled data filters as a function of GB are presented and compared. These root locus plots show both the desired and parasitic pole loci. It is concluded from these plots that stability of the analog filter does not guarantee stability of the derived sampled-data filter when the op amp effects are included even when stable mappings (mappings which are stable when the op amp's are ideal) are used (i.e., Bilinear Mapping). A comparison of the frequency response of the two second-order sampled-data filters is made with that of the continuous time filter from which they were derived which shows explicitly the combined effects of both the desired and parasitic poles and zeros.

Experimental results are presented and compared with the theoretically predicted performance. These show close agreement.

This is followed by the presentation of a method of analytically determining the op amp GB effects in SC filters employing any number of op amp's, capacitors, and switches.

II. DETERMINATION OF OPERATIONAL AMPLIFIER GB EFFECTS IN ACTIVE NETWORKS

All op amp's will be assumed to be ideal except for a frequency dependent gain

$$A(s) = \frac{GB}{s} \tag{1}$$

where GB is the gain-bandwidth product of the op amp. An ideal op amp is one in which $GB = \infty$.

If the op amp's in the macromodel of Fig. 1(b) are ideal, then it follows that both circuits in Fig. 1 have identical gains as well as input and output characteristics. This macromodel is basically the balanced time-constant integrator of Thomas [5] with buffered inputs and will be used for the theoretical analysis. Furthermore, it is convenient to adjust GB (with matched resistors) in the experi-

mental simulation of the single-pole op amp. If the pole in the model of the op amp is not assumed at the origin, but rather at ω_a, the macromodel in Fig. 1(b) can still be used provided resistors of value $= 1/C_0\omega_a$ are placed in parallel with C_{01} and C_{02}. The use of the macromodel is not essential for the following analysis and experimental verification but is rather used for convenience.
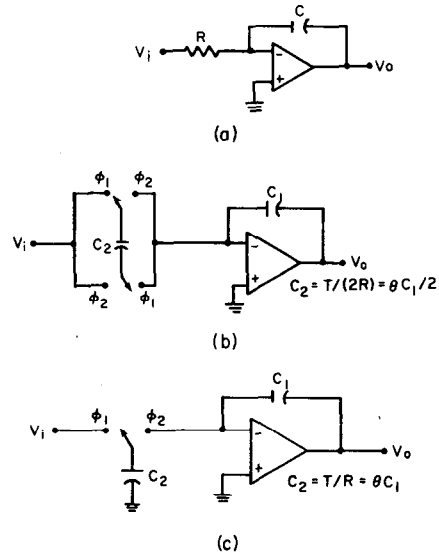
In SC circuits, all voltages are continuous functions of time between switching but many are discontinuous and undefined at the switch transitions. Throughout this paper all voltages are defined at any point in time by the right-hand limit

$$v(t) = \lim_{\varepsilon \to 0^+} v(t + \varepsilon). \tag{2}$$

Sampled-data points are obtained at integral multiples of T starting at $t = 0$. The clock phase ϕ_1 is always assumed to start at the same multiples of T. Often the value of the voltage immediately before a switch transition is also needed to analyze SC circuits. The notation

$$v(t^-) = \lim_{\varepsilon \to 0^-} v(t + \varepsilon) \tag{3}$$

will be used to denote the required left-hand limit. Obviously $v(t) = v(t^-)$ for all t between any two consecutive switch transitions due to the linear nature of the networks provided the switches are assumed to be ideal.

An important observation about the nodal output voltage of an op amp can be made from the macromodel of Fig. 1(b). Since the macromodel is an ideal differential integrator, it can be concluded that $v_0(t)$ is continuous for all time (i.e., no jumps occur at switch transitions) with bounded inputs.

A. Integrators

Two SC integrators are shown in Fig. 2 along with the basic analog integrator from which both are derived. The first SC integrator is noted for the bilinear-z transform

relationship from the s-domain to the z-domain if the op amp's are ideal. With ideal op amp's the second results in the popular forward z-transform [15].

It will be assumed that $v_i(t)$ is constant (sampled and held) for $(n-1)T \leqslant t < nT$. In general, this assumption is required to assure the circuit acts as a linear sampled-data system.

The transfer function of these two sampled-data integrators which includes the effects of the single pole of the op amp will be denoted, respectively, by $I_1(z)$ and $I_2(z)$. Using an analysis similar to that of Temes [13], it follows that the first transfer function may be expressed as

$$I_1(z) = \frac{-\dfrac{c_2}{c_1}(1+z^{-1})(1-e^{aT})z^{-1}}{(1-z^{-1})\left(1+e^{aT}\cdot\dfrac{c_2-c_1}{c_2+c_1}z^{-1}\right)} \qquad (4)$$

where $a = -GBc_1/c_1 + c_2$. Note that for unity gain ($c_2 = c_1$) the parasitic pole introduced by the op amp disappears. By applying the bilinear z-transform directly to the analog integrator transfer function *in the case the op amp's are ideal* one obtains

$$I_{1,\text{ideal}}(z) = -\frac{c_2}{c_1}\frac{1+z^{-1}}{1-z^{-1}}. \qquad (5)$$

Note that this is *not* the limit as $GB \to -\infty$ (alt. $a \to -\infty$) of $I_1(z)$ (they actually differ by one time delay z^{-1}). This is, however, expected since for *any* finite gain–bandwidth product, GB, the op amp outputs can not jump instantaneously after the clock transition so the limit will not jump either.

By a similar procedure $I_2(z)$ is found to be

$$I_2(z) = -\frac{c_2}{c_1}\frac{z^{-1}}{1-z^{-1}}\frac{1-e^{\frac{aT}{2}}\left[1-\dfrac{c_2}{c_1+c_2}(1-e^{a_1T/2})z^{-1}\right]}{1-\dfrac{c_1}{c_1+c_2}e^{(a+a_1)T/2}z^{-1}} \qquad (6)$$

where $a = -GBc_1/c_1 + c_2$ and $a_1 = -GB$. Again, this can be compared to the expression which is found in the ideal op amp case

$$I_{2,\text{ideal}}(z) = \frac{-\dfrac{c_2}{c_1}}{z-1}. \qquad (7)$$

Note that this is the limit as $GB \to \infty$ of $I_2(z)$. Because of the nature of the two phase clock employed in the integrator, integrator outputs in the ideal case are discontinuous only at $1/2 + kT$, $k\varepsilon\{0,1,\cdots\}$ and are continuous at $t = kT$, $k\varepsilon\{0,1,\cdots\}$. Thus no additional delay is expected in this case.

An investigation of (4) and (6) seems to indicate that for practical values of GB and T, these equations differ very little from (5) and (7). It can be readily shown, however, that these small differences are comparable in magnitude to those which occur when the GB effects are included in the analysis of the parent analog integrator from which
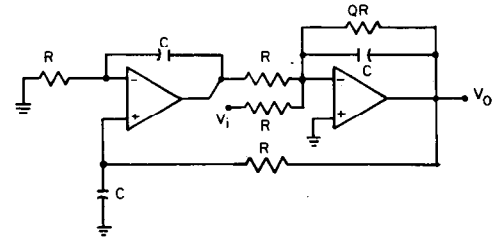
(a)
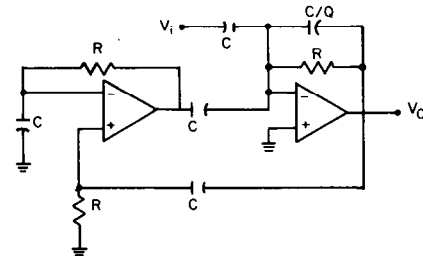
(b)

Fig. 3. Second-order analog bandpass filters. (a) Conventional. (b) Minimum resistor.

they were derived. Furthermore, the increased order in the transfer functions due to the op amp's causes additional phase shift which may ultimately affect stability in feedback structures.

The differences in the performance of the analog integrators from ideal are known to strongly affect the performance of analog filters [6], [18], [19]. It is shown in the next section that the deviations in (4) and (6) likewise cause serious degradation in performance when these integrators are used in analog sampled-data filters.

At this point the temptation exists to analyze filters employing these integrators in terms of flow-diagrams and the integrator gains of (4) and (6) as is done for continuous time filters and ideal sampled-data filters. Unfortunately this method of analysis cannot be used in general since the integrator outputs (which often are actually inputs to the next integrator) do not remain constant throughout the interval $([n-1]T, nT)$ which was required to obtain (4) and (6). A sample-and-hold could be employed to each integrator output to hold the voltage constant throughout the interval but this would cause excessive delay through the filter and seriously degrade performance. An analysis of higher order filters follows.

B. Bandpass Sampled-Data Filters

A second-order integrator-based bandpass filter is shown in Fig. 3(a). This analog filter and the subsequently derived sampled-data filters were selected because they are topologically relatively simple but serve as good examples for developing the general method of analysis presented in the following section as well as serving as an excellent example for demonstrating the importance of considering GB product effects when designing analog sampled-data filters. This filter, which is similar to that of Geffe [17], uses an inverting and noninverting integrator in a loop and only two op amp's.

The transfer function of this analog filter with ideal op

(a)

$$C_1 = C_3 = C$$
$$C_2 = C_5 = T/R = C\theta$$
$$C_4 = T/(QR) = C\theta/Q$$

(b)

$$C_1 = C_2 = C_3 = C_5 = C$$
$$C_4 = C/Q$$
$$C_6 = C_7 = C_8 = T/(2R) = C\theta/2$$
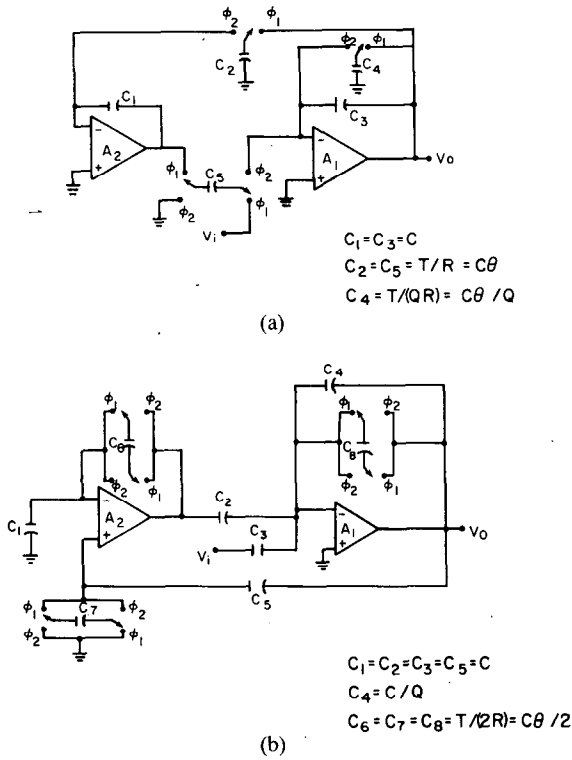
Fig. 4. Sampled-data bandpass filters. (a) Forward. (b) Bilinear.

amp's is

$$T(s) = \frac{-s\omega_0}{s^2 + s\frac{\omega_0}{Q} + \omega_0^2} \qquad (8)$$

where $\omega_0 = 1/RC$.

A sampled-data filter derived from this analog filter is shown in Fig. 4(a). This filter uses the Forward Integrator discussed earlier in conjunction with the inverting-summing switching scheme of [15].

A bilinear switching transformation of this analog filter is also desired due to the attractive properties of the bilinear s-plane to z-plane transformation. Because of the large number of resistors in this analog filter, a considerable number of SC's are required to convert this to a sampled-data filter using the bilinear switching scheme of Temes et al. [16]. If a low-pass to high-pass transformation followed by a frequency dependent scaling is made on the analog circuit, the circuit can be transformed to the minimum resistor configuration [8] of Fig. 3(b). The transfer function of the latter circuit is also given by (8). The sampled-data filter derived from Fig. 3(b) obtained by replacing the resistors with the bilinear SC's is shown in Fig. 4(b). The circuit of Fig. 4(b) will now be analyzed.

For $(n-1)T \leqslant t < nT$, the circuit of Fig. 4(b) is linear and can be redrawn as in Fig. 5 where the voltages $e_i(t)$, $i = 1, \cdots, 8$ are the capacitor voltages at time t. From the macromodel of the op amp's it follows that

$$v_2(t) = -GB_2 \int_{nT-T}^{t} \left(v_a(\tau) - v_b(\tau) \right) d\tau + v_2(nT - T) \qquad (9)$$

Fig. 5. Circuit of Fig. 4(b) for $nT - T < t < nT$.

and

$$v_0(t) = -GB_1 \int_{nT-T}^{t} v_c(\tau) d\tau + v_0(nT - T). \qquad (10)$$

From conservation of charge it follows that

$$v_a(t) = \frac{c_6}{c_1 + c_6} v_2(t) + \frac{c_1}{c_1 + c_6} v_2[nT - T] - e_6[nT - T] \qquad (11)$$

$$v_b(t) = \frac{c_5}{c_5 + c_6} v_0(t) + \frac{c_7}{c_5 + c_7} v_0[nT - T] - e_5[nT - T] \qquad (12)$$

and

$$v_c(t)$$
$$= \frac{c_2(v_2(t) - v_2[nT - T]) + (c_4 + c_8)(v_0(t) - v_0[nT - T])}{c_2 + c_3 + c_4 + c_8}$$
$$+ v_i[nT - T] - e_3[nT - T]. \qquad (13)$$

Define

$$v(t) = \begin{pmatrix} v_2(t) \\ v_0(t) \end{pmatrix} \qquad (14)$$

$$e(t) = \begin{pmatrix} e_3(t) \\ e_5(t) \\ e_6(t) \end{pmatrix} \qquad (15)$$

$$A = \begin{pmatrix} \dfrac{-c_6}{c_1 + c_2} & \dfrac{c_5}{c_5 + c_7} \\ \dfrac{-c_2}{c_2 + c_3 + c_4 + c_8} & \dfrac{-(c_4 + c_8)}{c_2 + c_3 + c_4 + c_8} \end{pmatrix} \qquad (16)$$

$$G = \begin{pmatrix} GB_2 & 0 \\ 0 & GB_1 \end{pmatrix} \qquad (17)$$

$$B_1 = \begin{pmatrix} 0 & -1 & 1 \\ 1 & 0 & 0 \end{pmatrix} \qquad (18)$$

and

$$C_1 = \begin{pmatrix} 0 \\ -1 \end{pmatrix} \qquad (19)$$

and

$$D_1 = \begin{pmatrix} \dfrac{-c_1}{c_1 + c_6} & \dfrac{c_7}{c_5 + c_7} \\[2ex] \dfrac{c_2}{c_2 + c_3 + c_4 + c_8} & \dfrac{(c_4 + c_8)}{c_2 + c_3 + c_4 + c_8} \end{pmatrix} . \quad (20)$$

Equations (9) and (10) may be expressed as

$$\frac{dv(t)}{dt} = G\big(Av(t) + B_1 e[nT - T] + C_1 v_i[nT - T] + D_1 v[nT - T]\big). \quad (21)$$

This differential equation can be solved to yield

$$v(t) = e^{GA(t - nT + T)} v[nT - T] + \big(e^{GA(t - nT + T)} - I\big)$$
$$\cdot A^{-1}[B_1 e[nT - T] + C_1 v_i[nT - T] + D_1 v[nT - T]] \quad (22)$$

where $e^{GA(t - nT + T)}$ is the fundamental matrix of (21). Since $v(t)$ is continuous at $t = nT$, (22) can be evaluated at $t = nT$ to obtain $v(nT)$. Following this evaluation and taking the z-transform we obtain

$$\big[zI - e^{GAT} - (e^{GAT} - I)A^{-1}D_1\big]V$$
$$= (e^{GAT} - I)A^{-1}[B_1 E + C_1 V_i] \quad (23)$$

where upper case variables again denote the z-transform of the corresponding lower case variables and I is the identity matrix. By conservation of charge during the switch transitions at nodes labeled v_a, v_0, and v_c it follows that

$$e_3(nT) = \left(\frac{c_2 + c_3 + c_4 - c_8}{c_2 + c_3 + c_4 + c_8}\right) e_3[nT - T] + \frac{c_2(c_2 + c_3 + c_4 - c_8)}{(c_2 + c_3 + c_4 + c_8)^2}\big(v_2[nT - T] - v_2[nT]\big)$$
$$+ \frac{(c_2 + c_4 + c_8)v_i(nT) - (c_2 + c_4 - c_8)v_i(nT - T)}{c_2 + c_3 + c_4 + c_8} + \frac{(c_4 + c_8)(c_2 + c_3 + c_4 - c_8)}{(c_2 + c_3 + c_4 + c_8)^2} \cdot v_0[nT - T]$$
$$+ \left(\frac{-2c_8(c_2 + c_3 + c_4 + c_8) - (c_4 + c_8)(c_2 + c_3 + c_4 - c_8)}{(c_2 + c_3 + c_4 + c_8)^2}\right) \cdot v_0(nT) \quad (24)$$

$$e_5(nT) = \left(\frac{c_5 - c_7}{c_5 + c_7}\right) e_5(nT - T) + \frac{c_7(c_7 - c_5)}{(c_7 + c_5)^2} v_0(nT - T)$$
$$+ \frac{c_7(3c_5 + c_7)}{(c_5 + c_7)^2} v_0(nT) \quad (25)$$

$$e_6(nT) = \left(\frac{c_1 - c_6}{c_1 + c_6}\right) e_6[nT - T]$$
$$+ \frac{c_1(c_1 - c_6)}{(c_1 + c_6)^2}[v_2(nT) - v_2[nT - T]]. \quad (26)$$

Define

$$B_2 = \begin{bmatrix} \dfrac{c_2 + c_3 + c_4 - c_8}{c_2 + c_3 + c_4 + c_8} & 0 & 0 \\[2ex] 0 & \dfrac{c_5 - c_7}{c_5 + c_7} & 0 \\[2ex] 0 & 0 & \dfrac{c_1 - c_6}{c_1 + c_6} \end{bmatrix} \quad (27)$$

$$B_3 = \begin{bmatrix} \dfrac{-c_2(c_2 + c_3 + c_4 - c_8)}{(c_2 + c_3 + c_4 + c_8)^2} & \dfrac{-2c_8(c_2 + c_3 + c_4 + c_8) - (c_4 + c_8)(c_2 + c_3 + c_4 - c_8)}{(c_2 + c_3 + c_4 + c_8)^2} \\[3ex] 0 & \dfrac{c_7(c_7 + 3c_5)}{(c_7 + c_5)^2} \\[3ex] \dfrac{c_1(c_1 - c_6)}{(c_1 + c_6)^2} & 0 \end{bmatrix} \quad (28)$$

$$B_4 = \begin{bmatrix} \dfrac{(c_2 + c_3 + c_4 - c_8)c_2}{(c_2 + c_3 + c_4 + c_8)^2} & \dfrac{(c_4 + c_8)(c_2 + c_3 + c_4 - c_8)}{(c_2 + c_3 + c_4 + c_8)^2} \\[3ex] 0 & \dfrac{c_7(c_7 - c_5)}{(c_5 + c_7)^2} \\[3ex] -\dfrac{c_1(c_1 - c_6)}{(c_1 + c_6)^2} & 0 \end{bmatrix} \quad (29)$$

$$B_5 = \begin{bmatrix} \dfrac{c_2 + c_4 + c_8}{c_2 + c_3 + c_4 + c_8} \\[2ex] 0 \\[1ex] 0 \end{bmatrix} \quad B_6 = \begin{bmatrix} \dfrac{c_8 - c_2 - c_4}{c_2 + c_3 + c_4 + c_8} \\[2ex] 0 \\[1ex] 0 \end{bmatrix} . \quad (30)$$

It follows from (24)–(30) that

$$e(nT) = B_2 e[nT - T] + B_3 v(nT) + B_4 v[nT - T]$$
$$+ B_5 v_i(nT) + B_6 v_i[nT - T]. \quad (31)$$

Taking the z-transform of (31) it follows that

$$E = (zI - B_2)^{-1}\big[(B_3 zI + B_4)V + (B_5 zI + B_6)V_i\big]. \quad (32)$$

Substituting (32) into (23) one obtains

$$V = M^{-1}\big[(e^{GAT} - I)A^{-1}\big(B_1(zI - B_2)^{-1}$$
$$\cdot (B_5 zI + B_6) + C_1\big)\big]V_i \quad (33)$$

where

$$M = zI - e^{GAT} - (e^{GAT} - I)A^{-1}$$
$$\cdot \left(D_1 + B_1(zI - B_2)^{-1}(B_3zI + B_4) \right). \quad (34)$$

The transfer function, $H(z)$, is thus the second entry in the coefficient vector of (33). A closed-form symbolic expression of $H(z)$ as a ratio of polynomials appears quite unwieldly. However, for a given capacitor ratio and sampling interval the transfer function can be obtained. With the aid of a digital computer, plots of $|H(z)|$, $\llcorner H(z)$ and the pole and zero locations can be readily obtained. Root locus and transfer function magnitude plots for both circuits of Fig. 4 are discussed later. A time-domain response can also be obtained for this filter if desired by investigating (22).

The transfer function for the circuit of Fig. 4(a) is given by the first entry in the vector $M_1^{-1}M_2$, where M_1 and M_2 are defined in (35) and (36). The derivation is similar to that just presented with the modifications outlined in a following section.

$$M_1(1,1) = \frac{c_2}{c_1}\left(e^{a_{01}T/2} - e^{T/2(a_2+a_{01})}\right)$$

$$M_1(1,2) = z - e^{T/2(a_2+a_{02})}$$

$$M_1(1,3) = e^{T/2(a_2+a_{02})} - 1$$

$$M_1(1,4) = \frac{c_2}{c_1}\left(1 - e^{a_{01}T/2}\right)\left(1 - e^{a_2T/2}\right)$$

$$M_1(2,1) = z - e^{a_{01}T/2}\left[\frac{c_3+c_4}{c_3}e^{a_1T/2} - \frac{c_4}{c_3}\right]$$

$$M_1(2,2) = \frac{c_5}{c_3}\left(e^{a_{02}T/2}\right)\left(e^{a_1T/2} - 1\right)$$

$$M_1(2,3) = \frac{c_5}{c_3}\left(e^{a_{01}T/2} - 1\right)\left(e^{a_{02}T/2} - 1\right)$$

$$M_1(2,4) = \frac{c_3+c_4}{c_3}e^{a_1T/2}\left(e^{a_{01}T/2} - 1\right)$$
$$+ \frac{c_4}{c_3}\left(1 - e^{a_{01}T/2}\right) + \left(e^{a_1T/2} - 1\right)$$

$$M_1(3,1) = \frac{c_2}{c_1+c_2}e^{a_{01}T/2}$$

$$M_1(3,2) = -\frac{c_2}{c_1+c_2}z$$

$$M_1(3,3) = z - \frac{c_1}{c_1+c_2}$$

$$M_1(3,4) = -\frac{c_2}{c_1+c_2}\left(e^{a_{01}T/2} - 1\right)$$

$$M_1(4,1) = \frac{z(c_4+c_5)}{(c_3+c_4+c_5)} - \frac{c_4}{c_3+c_4+c_5}e^{a_{01}T/2}$$

$$M_1(4,2) = \frac{c_5}{c_3+c_4+c_5}e^{a_{02}T/2}$$

$$M_1(4,3) = \frac{c_5}{c_3+c_4+c_5}\left(1 - e^{a_{02}T/2}\right)$$

$$M_1(4,4) = -z + \frac{c_3+c_4\left(e^{a_{01}T/2} - 1\right)}{c_3+c_4+c_5}.$$

$$(35)$$
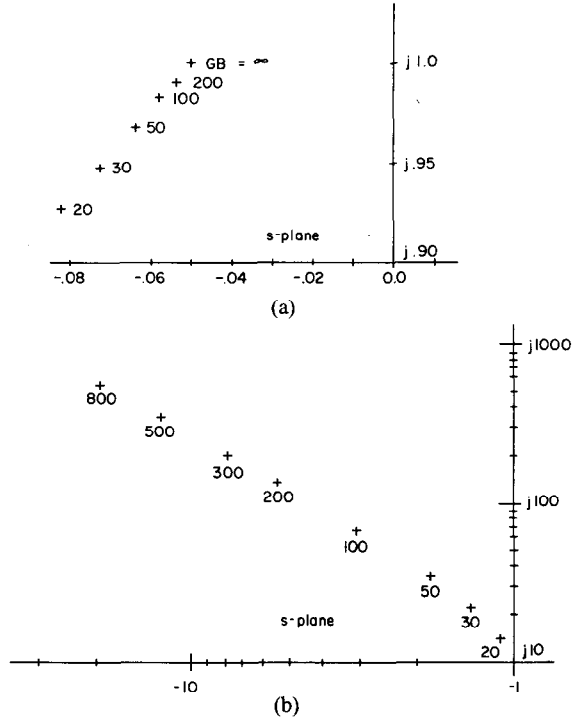
Fig. 6. Poles of analog filter of Fig. 3(b) GB_n values indicated on plot. (a) Desired poles. (b) Parasitic poles.

$$M_2 = \begin{bmatrix} 0 \\ \dfrac{c_5}{c_3}\left(e^{a_1T/2} - 1\right) \\ 0 \\ \dfrac{c_5}{c_3+c_4+c_5} \end{bmatrix} \quad (36)$$

where

$$a_{01} = -GB_1$$
$$a_{02} = -GB_2$$
$$a_1 = \frac{-c_3(GB_1)}{c_3+c_4+c_5}$$
$$a_2 = \frac{-c_1GB_2}{c_1+c_2}. \quad (37)$$

III. OPERATIONAL AMPLIFIER EFFECTS ON PERFORMANCE OF ANALOG SAMPLED DATA FILTERS

In this section a comparison of the performance of the analog bandpass filter of Fig. 3 is made with that of the two derived SC filters of Fig. 4. A design pole Q of 10 is assumed throughout. The symbol ω_0 (rad/s) denotes the design center frequency of the bandpass filters and T the time between sampled-data points. The normalized GB product is defined by $GB_n = GB/\omega_0$. A comparison of the pole locus as a function of GB is made for these three circuits. The pole locus plots are in the s-plane for the analog filter and in the z-plane for the sampled-data filters. These are followed by plots of the transfer function magnitudes for several values of GB_n. Fig. 6 shows a plot of the upper half-plane desired and parasitic poles for the analog
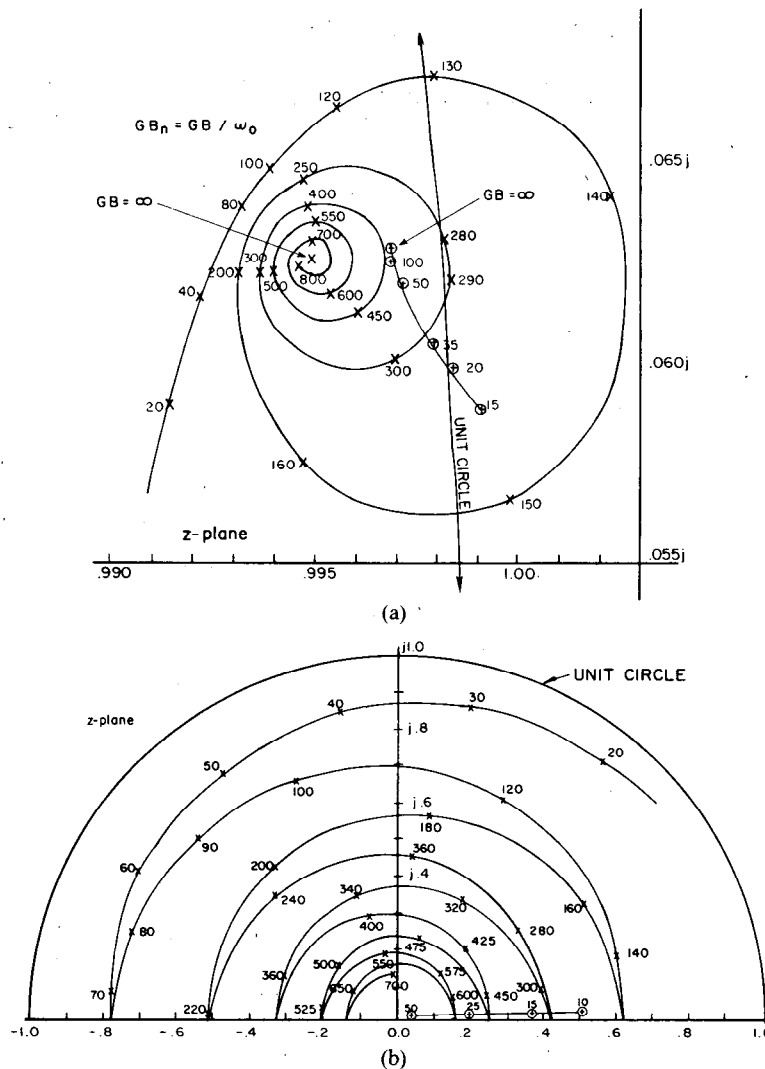
Fig. 7.   Poles of sampled-data filters $\theta = 0.01 \times 2\pi$, $GB_n = GB/\omega_0$ values indicated on plot. $\oplus$-circuit of Fig. 4(a). X-circuit of Fig. 4(b). (a) Desired poles. (b) Parasitic poles.

filter of Fig. 3. Figs. 7 and 8 are plots of the upper half plane desired and parasitic poles for values of $\theta = (0.01) 2\pi$ rad/s and $(0.05) 2\pi$ rad/s where $\theta = T\omega_0$. Note that the clock frequency for the switch control is related to θ by $f_c = \omega_0/\theta$ for the circuit of Fig. 4(a) and $f_c = \omega_0/2\theta$ for the circuit of Fig. 4(b). It should be noted that the $GB_n = \infty$ pole locations differ for the two filters of Fig. 4. This is due to the well-known fact that the pole locations are transformation dependent. The absence of pole locus plots for the circuit of Fig. 4(a) when $\theta = (0.05) \times 2\pi$ is due to the fact that this circuit is unstable with this slow switching rate even if the op amp's are ideal.

Several observations about the performance and stability of these filters can be made from the pole locus plots.

1) The value of GB_n required for stability of the analog filter is different than that for either of the sampled-data filters.

2) The pole locus and stability criterion for the SC filter appears to be strongly dependent upon the particular switching arrangement employed.

3) Larger values of θ (slower switch clock rates) significantly reduce op amp requirements as can be seen from a comparison of Figs. 7 and 8. This, however, is done the expense of increased warping in the s-plane to z-plane transformation. It is interesting to note that for $\theta = (0.01)$ 2π and $\theta = (0.05) 2\pi$ the sampled-data filter of Fig. 4(b) is unstable for certain values of GB_n whereas the analog filter from which it was derived remains stable.

4) The spiraling nature of the pole locus for the circuit of Fig. 4(b) is most interesting. It demonstrates that improving GB locally may well result in a deterioration in filter performance or actually cause instability. This phenomenon resembles the degradation of a digital filter's performance arising from a local increase in wordlength and roundoff errors. The cause of this spiraling locus can be traced to the time-domain equation (22) where the eigenvalues of the state transition matrix can be shown to have a relatively large imaginary component indicating a strongly underdamped system. This underdamping causes ringing transients in the time domain after switch transitions and

(a)

(b)
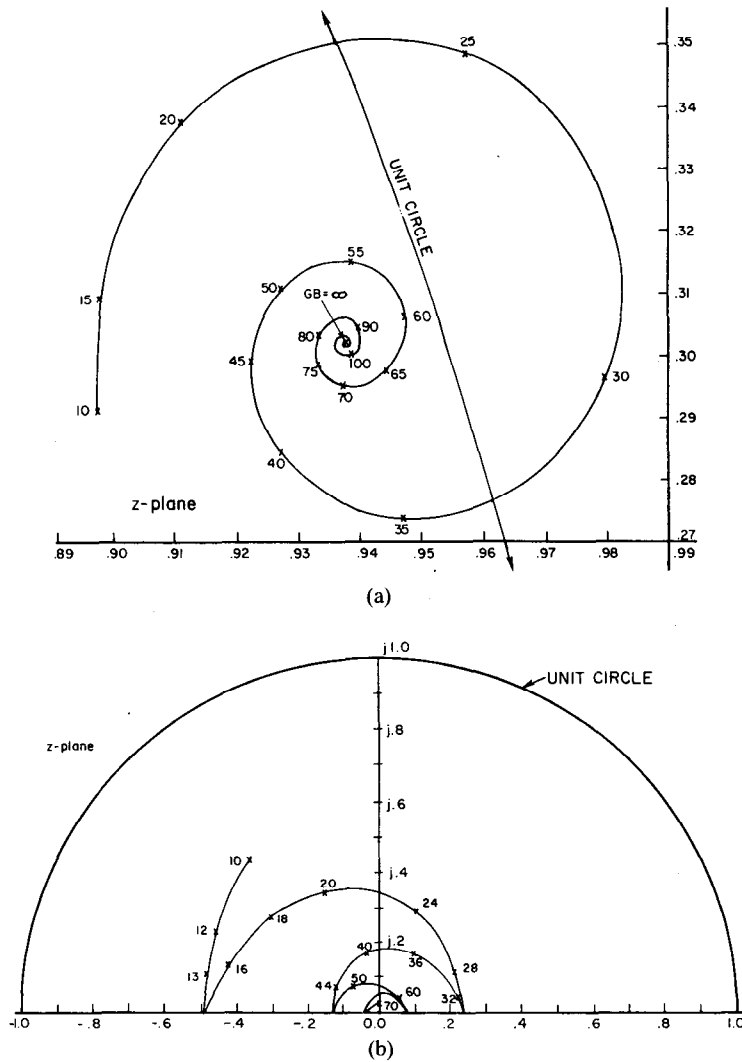
Fig. 8. Poles of sampled-data filters $\theta = 0.05 \times 2\pi$, $GB_n = GB/\omega_0$ values indicated on plot. X-circuit of Fig. 4(b). (a) Desired poles. (b) Parasitic poles.

these transients do not completely die out before the next switch transition which, in turn, makes the pole positions in the z-domain dependent upon the size of the ripple at the next transition. The eigenvalues for the circuit of Fig. 4(b) are real since during the linear operation intervals the filter is comprised of two disconnected first-order networks due to the switching arrangement employed.

5) The parasitic pole plots indicate no stability problems with either of these circuits. The inclusion of these plots is justified, however, since some analog filters which have desired poles in the left half-plane are actually unstable due to right half-plane [21] parasitic poles. A similar phenomenon might be expected in the sampled-data filters.

6) The spiraling nature of the desired poles can not be obtained by employing the finite gain model of the op amp.

The combined effects of the parasitic poles and desired poles as well as the zero locations which have not been discussed can be seen in the transfer function magnitude plots of Fig. 9. The plots show the gains $|T(j\omega)|$ and
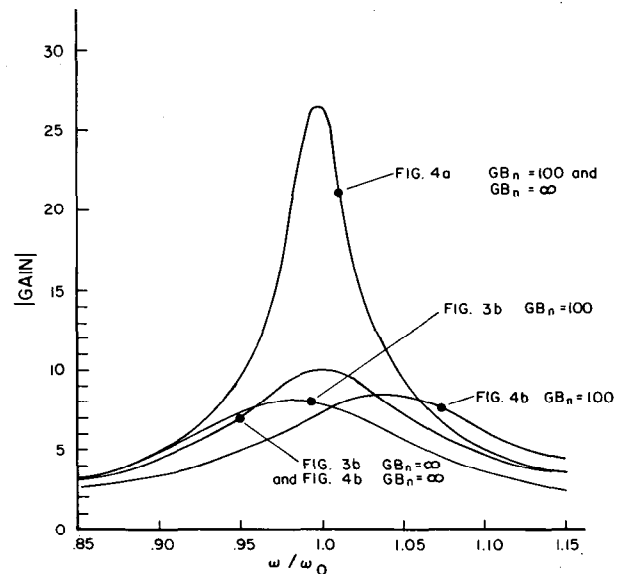
Fig. 9. Magnitude responses for sampled-data filters. $\theta = 0.01 \times 2\pi$, GB_n = 100 and ∞.

$|H(e^{j\omega})|$ for the analog and sampled-data circuits, respectively, on the same set of axes. The frequency axis has been chosen to cover the range of interest. The bilinear z-transformation mapping obtained from the circuit of Fig. 4(b) shows much less frequency warping than is obtained by the circuit of Fig. 4(a) as expected. One is cautioned that the pole plots should be considered in conjunction with the magnitude plots since the apparently good performance for some values of GB_n in Fig. 4 (e.g., $\theta = 0.01 \times 2\pi$, $GB_n = 100$) are only obtained because the pole locations on the spiral are locally close to the desired pole locations but this performance deteriorates rapidly for small changes of GB in either direction.

A comment about the assymtotic performance as $GB \to \infty$ of the sampled-data filters is in order. The circuit of Fig. 4(a) actually has two parasitic poles and two parasitic zeros which all converge to $z = 0$. Thus the transfer function converges to that obtained by initially assuming the op amp's to be ideal as was the case for the integrator of Fig. 2(b) from which this circuit was derived. The circuit of Fig. 4(b) has a single parasitic zero and two parasitic poles all of which converge to zero indicating a single extra z remains in the denominator of the limit of the transfer function (when compared to that obtained by initially assuming the op amp's to be ideal) as was the case for the integrator of Fig. 2(c) from which this circuit was derived.

IV. GENERAL SWITCHED-CAPACITOR FILTER ANALYSIS

A general SC filter employing any number of op amp's modeled by the single-pole model in which all nodes contain an op amp input or output (not necessarily matched) and no nonlinear operation for $nT - T < t < nT$ can be analyzed by the procedure previously followed where only the dimensions and entries in the A, B, C, and G matrices and v and e vectors differ. The procedure is outlined below.

1) Write the differential equations governing the operation of each op amp using the macromodel of Fig. 1. The differential equation can always be written in the form shown in (21) where the dimension of v corresponds to the number of op amp's.

2) Obtain the solution of the differential equation and evaluation at $t = nT$ since the op amp output voltages are continuous functions of time.

3) Use conservation of charge principles at switching intervals to write the $e(t)$ vector in (31) in terms of $v(t)$ $v_i(t)$, and $e(nT - T)$.

4) Take the z-transform of the equations obtained in 2) and 3) and solve simultaneously to obtain the solution presented in (33).

In the case that the filter operation is not linear for $nT - T < t < nT$, the above analysis must be modified. Assume that the clocks are phased so that switching occurs k times in the interval $(nT - T, nT)$. There are now $k + 1$ subintervals over which circuit operation is linear. The analysis of sampled-data filters having multiphase clocking of the switches is outlined below.

1) Write a set of $k + 1$ differential equations governing the operation of the op amp's in each of the $k + 1$ subintervals.

2) Solve the $k + 1$ differential equations and evaluate at the right-hand endpoint of the corresponding subinterval. The op amp output voltages are all continuous functions of time.

3) Use conservation of charge at the switching transitions to obtain the $e(t)$ vectors.

4) Take the z-transform of the equations obtained in 2) and 3) and solve simultaneously to obtain $V_0(z)$ in terms of $V_i(z)$.

The economic advantages of conducting a closed form analysis of sampled-data filters should be obvious by investigating the computation required to solve equations such as (33). The total CPU time required to generate the data for all root locus and transfer function magnitude plots presented in this paper is well under 1 min on a Amdahl 460 V and no attempt was made to optimize the algorithms employed. Aside from the economic advantages when compared to existing time-domain approaches, *a time-domain analysis, which may even be based upon a single value of GB, may miss the spiraling motion such as was obtained for the circuit of Fig. 4(b) giving false encouragement for acceptable filter performance.*

V. EXPERIMENTAL RESULTS

A comparison of the theoretical performance predicted in the previous section is made with the experimental performance in this section.

The SC filter of Fig. 4(b) was designed for a center frequency of 200 Hz, $Q = 10$, and $\theta = (0.01)(2\pi)$. The low center frequency was picked so that the op amp's could be replaced by the macromodel of Fig. 1(b) which provides a convenient means of experimental GB adjustment with the resistors, R, in the macromodel. This macromodel provides the additional advantage of forcing additional amplifier poles far away from the effective value of GB thus making the single-pole gain approximation of (1) which was used for the theoretical analysis very good.

All op amp's were 741 type and the analog switches were HI201. Capacitors c_1, c_2, c_3, and c_5 were all matched to within 0.5 percent of 5.10 nF. Capacitors c_6, c_7, and c_8 were within 0.5 percent of 158 pF and the capacitors in the op amp macromodel were within 0.5 percent of 1.10 nF. The remaining experimental parameters were $c_4 = 515$ pF and $f_c = 10.14$ kHz. The resistors, R, in the op amp macromodel were matched to within 1 percent and satisfied the expression

$$R = \frac{7.22 \times 10^5}{GB_n}$$

where GB_n is the normalized GB product. No sample-and-hold was used at the input because of the relatively high sampling rate employed.

TABLE I
EXPERIMENTAL PERFORMANCE OF SWITCHED-CAPACITOR CIRCUIT
OF FIG. 4(B)

GB_n	f_o (Hz)	Q
20	200	4.0
40	209	4.6
80	218	5.3
100	225	6.3
120	230	6.8
140	244	6.25
141.6	248	12.4
144.4	254	46.
145	257	128
166	182	61
168	186	21
172	190	10
180	197	7

The measured value of the center frequency, f_0, and Q are listed in Table I for various values of GB_n. The value of Q was obtained by dividing f_0 by the measured 3-dB bandwidth. The circuit went into low-frequency oscillation (approx. 200 Hz) for $145 < GB_n < 166$. The circuit went into high-frequency oscillation (approx. 100 kHz) for $GB_n > 226$.

A comparison of the data in Table I with the pole locus of Fig. 7 shows the predicted increase in both center frequency and Q as GB_n increases from 20 to 120. The predicted unstable mode of operation ($130 < GB_n < 152$) was observed though shifted slightly ($145 < GB_n < 166$). The subsequent large drop in center frequency once stability is maintained by increasing GB_n followed by a decrease in Q and increase in f_0 was also observed.

The analog circuit of Fig. 3(b) from which the SC configuration was derived was also experimentally evaluated. The circuit was identical to that used in the SC evaluation with the exception that the switched-capacitor portions (c_6, c_7, and c_8) were replaced with matched resistors that were all within 0.5 percent of 157.5 kΩ. The experimental results closely paralelled the theoretical for $GB_n < 158$. For GB_n greater than 158 the circuit also went into high frequency oscillation (approx. 100 kHz). As predicted, the absence of the serious Q-enhancement and low-frequency oscillation that was present in the SC case was observed as well as the significantly reduced shift in center frequency.

The high-frequency oscillation obtained in both configurations is not predictable by the theoretical analysis but is due to the presence of additional poles not accounted for in the single-pole model of the op amp used in the analysis.

Using a more accurate two-pole model for the op amp's the parasitic poles were obtained for the analog configuration using the methods of [22]. One pair of these parasitic

poles appeared in the right half-plane. This instability was also observed experimentally using actual op amp's rather than the macromodel. This problem would not persist with most configurations and the single-pole model would be generally more than adequate.

VI. CONCLUSIONS

A method of incorporating the frequency dependent gain of an op amp into the analysis of SC filters has been presented. The method allows a closed form analytical method for the determination of the minimum GB values required for a predetermined amount of Q enhancement. This may permit designers to reduce the op amp requirements and possibly reduce the chip area.

A second-order bandpass analog filter was transformed to a SC configuration by employing two popular but different switching arrangements. It was shown in this example that the effects of switching rates, switching arrangements, and gain–bandwidth products of the op amp's interactively and significantly affect the performance of SC filters in frequency ranges where these filters are currently applied. Experimental results were presented which agreed closely with the theoretical results. It is shown in this example that the op amp effects can be more significant in SC filters than they are in the analog counterpart.

Although it is not our intention to imply other SC filters are as susceptable to op amp effects as are the ones presented here or that the bilinear-z transform switching arrangements is particularly affected by these parasitic effects it seems likely that a useful algorithm for analyzing SC filters must include a good frequency dependent model of the op amp's [22] since the spiraling pole locus which surfaced in the bilinear state variable filter is not obtainable with the more popular finite-gain model. The failure to appropriately consider GB product effects or underestimate their relative significance when compared to other nonideal characteristics may lead to either a serious degradation in filter performance or instability as evidenced both theoretically and experimentally by one of the examples presented.

REFERENCES

[1] A. S. Sedra and J. L. Espinoza, "Sensitivity and frequency limitations of biquadratic active filters," *IEEE Trans. Circuits Syst.*, vol. CAS-22, pp. 122–130, Feb. 1975.
[2] A. Budak and D. M. Petrela, "Frequency limitations of active filters using operational amplifiers," *IEEE Trans. Circuit Theory*, vol. CT-19, pp. 322–328, July 1972.
[3] R. Geiger and A. Budak, "Active filters with zero amplifier sensitivity," *IEEE Trans. Circuits Syst.*, vol. CAS-26, pp. 277–288, Apr. 1979.
[4] D. Akerberg and K. Mossberg, "A versatile active RC building block with inherent compensation for the finite bandwidth of the amplifier," *IEEE Trans. Circuits Syst.*, vol. CAS-21, pp. 75–78, Jan. 1974.
[5] L. Thomas, "The biquad: Part I—Some practical design considerations," *IEEE Trans. Circuit Theory*, vol. CT-18, pp. 350–357, May 1971.
[6] P. Brackett and A. Sedra, "Active compensation for high-frequency effects in op amp circuits with applications to active RC filters," *IEEE Trans. Circuits Syst.*, vol. CAS-23, pp. 68–72, Feb. 1976.
[7] Y. P. Tsividis, "Analysis of switched capacitive networks," *IEEE Trans. Circuits Syst.*, vol. CAS-26, pp. 935–947, Nov. 1979.

[8] M. L. Liou and Y. L. Kuo, "Exact analysis of switched capacitor circuits with arbitrary inputs," *IEEE Trans. Circuits Syst.*, vol. CAS-26, pp. 213–223, Apr. 1979.

[9] C. F. Kurth and G. S. Moschytz, "Nodal analysis of switched-capacitor networks," *IEEE Trans. Circuits Syst.*, vol. CAS-26, pp. 93–105, Feb. 1979.

[10] F. Brglez, "Exact nodal analysis of switched capacitor networks with arbitrary switching sequences and general inputs—Part I," *Proc. Twelfth Annual Asilomar Conf. Circuits, Systems, and Computers*, Pacific Grove, CA, Nov. 1978.

[11] C. F. Lee and W. K. Jenkins, "Computer aided analysis of switched capacitor filters," in *Proc. Thirteenth Asilomar Annual Conf. Circuits, Systems, and Computers*, Pacific Grove, CA, Nov. 1979.

[12] K. Martin and A. S. Sedra, "Effects of the op amp finite gain and bandwidth on the performance of switched capacitor filer," *Proc. IEEE ISCAS/80*, Houston, TX, Apr. 1980.

[13] G. C. Temes, "Finite amplifier gain and bandwidth effects in switched-capacitor filters," *IEEE J. Solid-State Circuits*, vol. SC-15, pp. 358–361, June 1980.

[14] K. Martin and A. S. Sedra, "Strays-Insensitive switched-capacitor filters based on the bilinear z-transform," *Electron. Lett.*, vol. 15, pp. 365–366, June 1979.

[15] B. J. Hosticka, R. W. Brodersen and P. R. Gray, "MOS sampled data recursive filters using switched capacitor integrators," *IEEE J. Solid-State Circuits*, vol. SC-12, pp. 600–608, Dec. 1977.

[16] G. C. Temes, H. J. Orchard and M. Jahanbegloo, "Switched-Capacitor filter design using the bilinear z-transform," *IEEE Trans. Circuits Syst.*, vol. CAS-25, pp. 1039–1044, Dec. 1978.

[17] P. Geffe, "RC-Amplifier resonators for active filters," *IEEE Trans. Circuit Theory*, vol. CT-15, pp. 415–419, Dec. 1968.

[18] A. Soliman and M. Ismail, "On the active compensation of noninverting integrators," *Proc. IEEE*, vol. 67, pp. 962–963, June 1979.

[19] W. Kellner, "Noninverting integrators with improved high frequency response," *Electron. Lett.*, vol. 15, pp. 257–258, Apr. 1979.

[20] S. K. Mitra, *Analysis of Synthesis of Linear Active Networks*. New York:Wiley, 1969.

[21] R. Geiger, "Parasitic pole approximation techniques for active filter design," *IEEE Trans. Circuits Syst.*, vol. CAS-27, pp. 793–799, Sept. 1980.

[22] E. Sanchez-Sinencio and M. Majewski, "A nonlinear macromodel of operational amplifiers in the frequency domain," *IEEE Trans. Circuits Syst.*, vol. CAS-26, pp. 395–402, June 1979.

Randall L. Geiger (S'75–M'77) was born in Lexington, NE, on May 17, 1949. He received the B.S. degree in electrical engineering and the M.S. degree in mathematics from the University of Nebraska, Lincoln, in 1972 and 1973, respectively. He received the Ph.D. degree in electrical engineering from Colorado State University, Fort Collins, in 1977.

He joined the Faculty of the Department of Electrical Engineering at Texas A & M University, College Station, in 1977 and currently holds the rank of Associate Professor. His present research is in the area of active circuits, sampled data circuits, and microelectronics.

Dr. Geiger is a member of Eta Kappa Nu, Sigma Xi, Pi Mu Epsilon, and Sigma Tau.

✦
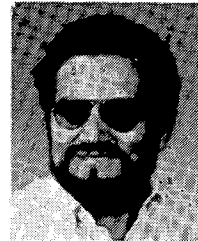
Edgar Sánchez-Sinencio (S'72–M'74) was born in Mexico City, Mexico, on October 27, 1944. He received the degree in communications and electronic engineering (professional degree) from the National Polytechnic Institute of Mexico, Mexico City, the M.S.E.E. degree from Stanford University, Stanford, and the Ph.D. degree from the University of Illinois at Champaign–Urbana, in 1966, 1970, and 1973, respectively.

In 1974 he held an industrial Post-Doctoral position with the Central Research Laboratories, Nippon Electric Company, Ltd., Kawasaski, Japan. He was a Visiting Professor in the Department of Electrical Engineering at the Texas A & M University during the academic year of 1979–1980. In 1975 he joined the Department of Electronics at the National Institute of Astrophysics, Optics and Electronics, Puebla, Mexico, where he is currently Professor and Head of the Department. His research interests include analog sampled-data filters, integrated circuits, and digital processing of signals.

Topological Formulations for the Coefficient Matrices of State Equations for Switched-Capacitor Networks

MAMORU TANAKA AND SHINSAKU MORI, MEMBER, IEEE

Abstract —This paper describes new topological formulas for the coefficient matrices of the state equation for a switched-capacitor (SC) network. The topological formulas are derived from a differential state equation describing an RC network with resistances (R, r) of OFF- and ON-switches, respectively. Differing from historical nodal analyses, this method is useful for the exact analysis of large scale SC networks, because the use of inverse matrices is not required and each network-construction-change in each switching time interval is disposed by a switching diagonal matrix with diagonal binary elements "1" and "0" for ON- and OFF-switches, respectively. New characteristic matrices will be applied in order to obtain the coefficient matrices efficiently by using recursive equations, which are suitable for computer-aided analysis.

I. INTRODUCTION

A SWITCHED-CAPACITOR (SC) network constructed by using MOS switches, MOS capacitors, and MOS operational amplifiers has been recognized as a